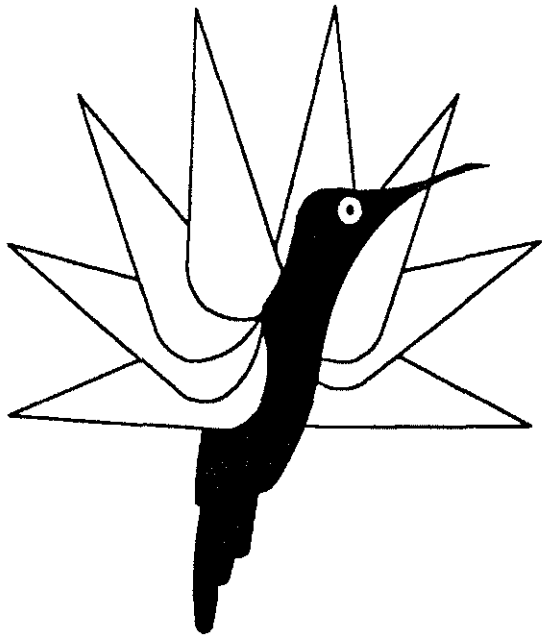

PAPER Nr. : 80

VALIDATION OF A FLIGHT MECHANICS MODEL USING FREQUENCY DOMAIN IDENTIFICATION RESULTS ON A SUPER PUMA HELICOPTER

BY

André-Michel Dequin

Paul Eglin

Aerodynamics Department
EUROCOPTER FRANCE

TWENTIETH EUROPEAN ROTORCRAFT FORUM
OCTOBER 4 - 7, 1994 AMSTERDAM

VALIDATION OF A FLIGHT MECHANICS MODEL USING FREQUENCY DOMAIN IDENTIFICATION RESULTS ON A SUPER PUMA HELICOPTER

André - Michel Dequin
and
Paul Eglin

Aerodynamics Department
Eurocopter France

Abstract

The first results of an ongoing validation of ECF generic simulation model S80 are presented.

Flight tests have been conducted with a Super Puma helicopter in forward flight between 100 and 140 Kt. An electronic device generated different kinds of input signals and, although the desired result was the open - loop transfer function of the unaugmented helicopter, a simple SAS was used to provide adequate stability, particularly at high speed.

Data was processed with identification tools developed by ONERA / CERT (Office National d'Etudes et de Recherches Aérospatiales / Centre d'Etudes et de Recherches de Toulouse), and a full set of transfer functions was determined in a 0.1 to 4 Hz frequency range.

The S80 simulation model is briefly presented. Linear simulation results are validated with respect to non - linear calculations and compared to the transfer functions that have been identified. Special attention is paid to cross couplings which are said to be poorly predicted by current models. This assessment must be tempered and some positive results can be shown.

The analysis of the contribution of main elements in the model gives a better understanding of model deficiencies. Some attempts are made to improve the quality of the simulation.

The first part of this work highlights some strengths points and weaknesses of the S80 simulation model. The first lesson to be learned, however, is that identification techniques can now be used in an industrial environment. It is possible to derive from flight measurements whatever theory is still unable to predict.

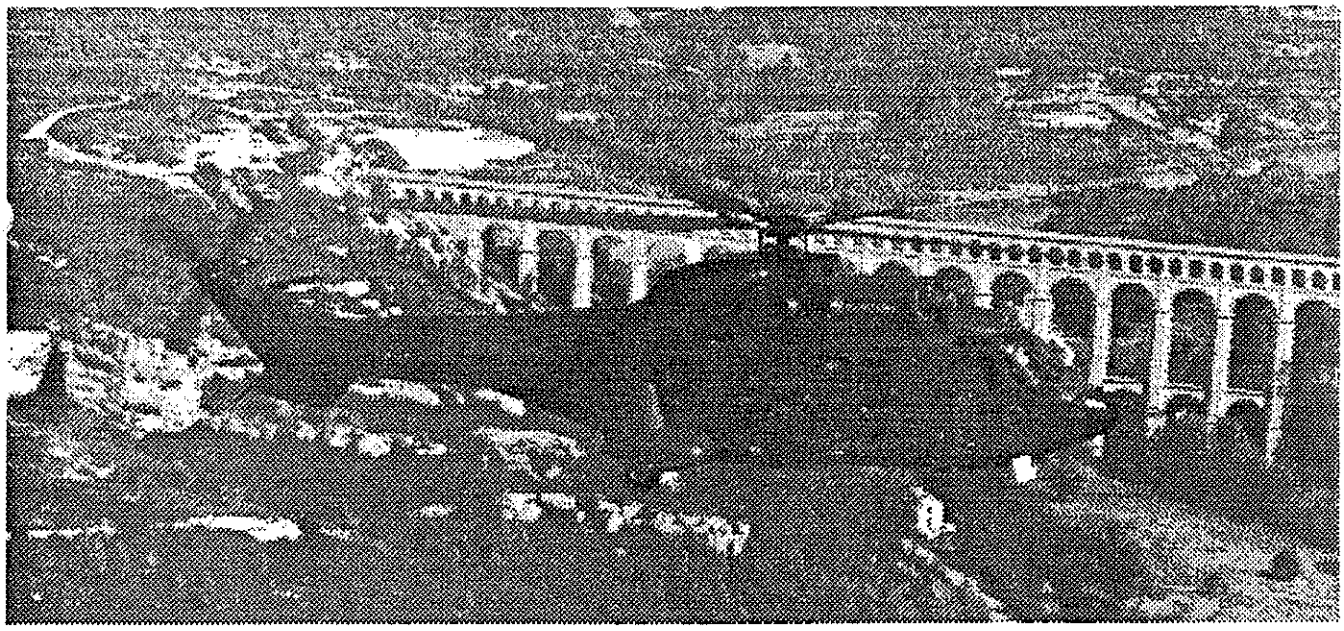

Figure 1: AS 332 L2 development helicopter

List of Symbols

p, q, r	roll, pitch and yaw rates about helicopter axes (deg/sec)
u,v,w	CG velocity components along helicopter axes (m/s)
φ,θ,ψ	fuselage attitudes (Euler angles)
δ_{lat}	lateral stick position (%)
δ_{lon}	longitudinal stick position (%)
δ_{ped}	pedal position (%)
δ_{col}	collective stick position (%)
ϕ	swashplate control phase angle (deg)
β_0	main rotor coning
β_{1c}	main rotor longitudinal flapping
β_{1s}	main rotor lateral flapping
δ_0	main rotor collective lag angle
δ_{1c}	main rotor cosine lag angle
δ_{ds}	main rotor sine lag angle
V_{i0}	mean induced velocity
$\mathcal{M}_y$	pitching moment in CG location
Ixx	roll inertia
Iyy	pitch inertia
Izz	yaw inertia
Ixz	product of inertia

Linear model: $\dot{X} = A.X + B.U$

X	state vector
A	stability matrix
U	control vector
B	control matrix

Abbreviations and Upper scripts:

MR	main rotor
TR	tail rotor
AF	airframe

Introduction

Validation has to accompany the development of any simulation model. The efforts must be equally shared between both activities, otherwise the resulting output can be of very poor use. When flight mechanics models are considered, validation has to deal with the three problem areas: trim, stability and response (1).

- Trim calculation is of primary interest during an helicopter development: performance, flight loads, control margins, static stability are dimensioning points directly linked to trim results. Trim validation was therefore addressed a long time ago and mainly consists in direct comparison of both calculated and flight measured parameters.

- Stability focuses on the estimation of the helicopter modes. They can be derived from flight data either by a complete identification of the stability matrix or simply by reading period and damping on fixed stick tests flight records. In simulation models, small perturbations methods or fixed stick calculations give comparable results.

- Response validation was first tackled through comparison of flight tests and simulation time histories: flight measured inputs, corrected by trim biases, are fed into the model and calculated behaviour compared to flight data. The main drawback of this procedure is its high sensitivity to trim quality and atmospheric perturbations: errors are integrated and rapidly lead to significant attitude differences. Repeatability is generally acceptable for on-axis results but can be questionable when off-axis response is considered. This procedure is therefore limited to very short tests, with simple, large amplitude inputs, looking mainly at on-axis response. In these conditions, current models are quite good and other methods have to be used when validation has to address more difficult problems.

Trim calculation in current models is not yet as good as would be expected and validation activities still have to be considered. However, simple tools have often been developed to compensate the lack of precision of physical simulation models in this area (performance calculations by energy methods for example).

As regards stability and response, comparison with flight is also not convincing. A large overestimation of Dutch roll damping is a common trend in state-of-the-art simulation models (1) and inter-axes couplings are all but understood (2). In this area, it is not so easy to develop simple models. Physical simulation models must then be used and therefore validated.

During the last years, non parametrical frequency domain identification was shown to offer broad validation possibilities. Transfer functions of the helicopter reflect both stability and response characteristics, cover off-axis as well as on-axis response and give valuable information in a large frequency range. All these points are of special interest when the use of the simulation model is foreseen for control laws development.

Since the tools developed by ONERA/CERT were available at ECF to process flight data, a study was started, which goals were:

1. to make flight tests on the Super Puma helicopter and derive from recorded flight data the transfer functions of the unaugmented helicopter in order to establish an experimental data base,

2. to validate the ECF simulation model within the whole frequency range, and especially to acquire a better knowledge of its ability to predict off-axis responses,

3. to improve, when possible, simulation results.

This activity was primarily research oriented. Nevertheless, the development of the NH 90 helicopter, similar in size and configuration to the AS 332 L2, was borne in mind during the definition of the test procedure. An accurate helicopter model is a key point in the design of a Fly By Wire control system and it was worth identifying deficiency areas in the ECF simulation model and being able to correct those from dedicated flight test results. An additional goal of this study was

4. to demonstrate that it was possible for ECF to use identification tools within a development process.

Flight tests identification procedure

The AS 332 L2 version is the last evolution of the Super Puma (fig. 1) which is a single main rotor, medium weight (9300 kg/20500 lb. max.) transport helicopter. Both main and tail rotors are four-bladed and equipped with ECF SPHERIFLEX articulated hubs.

The Flight Control System includes a conventional mechanical linkage between pilot inputs and hydraulic actuators of the main and tail rotor. This mechanical linkage includes a decoupling function between yaw axis and collective input.

The 4-axis Automatic Flight Control System (AFCS) is based on a Dual - Duplex digital computer. Among other features the AFCS contains a three-axis Stability Augmentation System (SAS) which performs feedback on attitude rates and consequently provides adequate damping on the three airframe axes.

The development model of the Super Puma L2 version has been used (fig. 1). This added some constraints (use of existing test installation, thus excluding measurements of main rotor parameters) but also offered interesting possibilities, such as the easily configurable digital auto pilot. These aspects will be similar in the NH90 case, as this was mandatory to make the reported work demonstrative in the perspective of this new development.

Test procedure

In order to provide the experimental data base for the validation activity, the open-loop transfer functions (both on-axis and off-axis) of the unaugmented AS 332L2 helicopter had to be derived from flight test measurements. Such tests are usually conducted with the stability augmentation system disengaged and inputs generated by the pilot. Different choices have been made within this activity:

1. An electronic device was developed to generate dynamic inputs. It allowed comparing the two different kinds of signals: the classical frequency sweep with increasing frequency and pseudo-random binary sequence (PRBS). Contrary to frequency sweeps, where low frequency occur at the beginning and high frequency at the end, frequencies in PRBS are better spread throughout the test duration. This kind of signal cannot be provided by the pilot alone and this explains the need for an electronic device. It has been implemented on one of the two autopilot channels.

2. The auto pilot was used and provided angular rate feedback on pitch, roll and yaw axes. The need was in the high speed range, included in the test envelope. In these conditions the stability of the natural helicopter is marginal and some level of augmentation to make tests easier is appreciated. The NH90 could be even more unstable: the use of the SAS was thus all the more interesting as the test procedure had to be applied during the development of this helicopter.

The input signals tested generally covered a frequency range from 0.1 to 2 Hz. However, some tests were continued up to 4 Hz in order to catch the main rotor first lead-lag mode. Both frequency sweep and PRBS signals and associated rate responses are presented on fig. 2. AS 332 L2 AFCS is a complex system including a large number of functions (attitude hold, stability augmentation, decoupling...). For these tests, taking advantage of the easily configurable AFCS, only the three-axis SAS (angular rates feedback) was used and all non-linearities were cancelled. It helped the pilot adhere to the flight configuration without counteracting or distorting the input signal excessively.

The pilot selected one axis on the input generator, trimmed the helicopter in the required flight conditions, SAS ON, and then started the test run. Pilot inputs were as limited as possible but had to prevent the helicopter from moving too much away from the trim conditions. The four axes (longitudinal and lateral stick, pedal and collective) of the helicopter were successively excited. One of the AFCS channels was used to connect the input generator.

As a result of AFCS operation the total signal on the rotors is the sum of the pilot, AFCS and input generator contributions (fig. 3). The selective effect of the SAS can be more easily observed on the frequency sweep curves: the amplitude of the low frequencies input is reduced by the SAS, as seen on fig. 2.

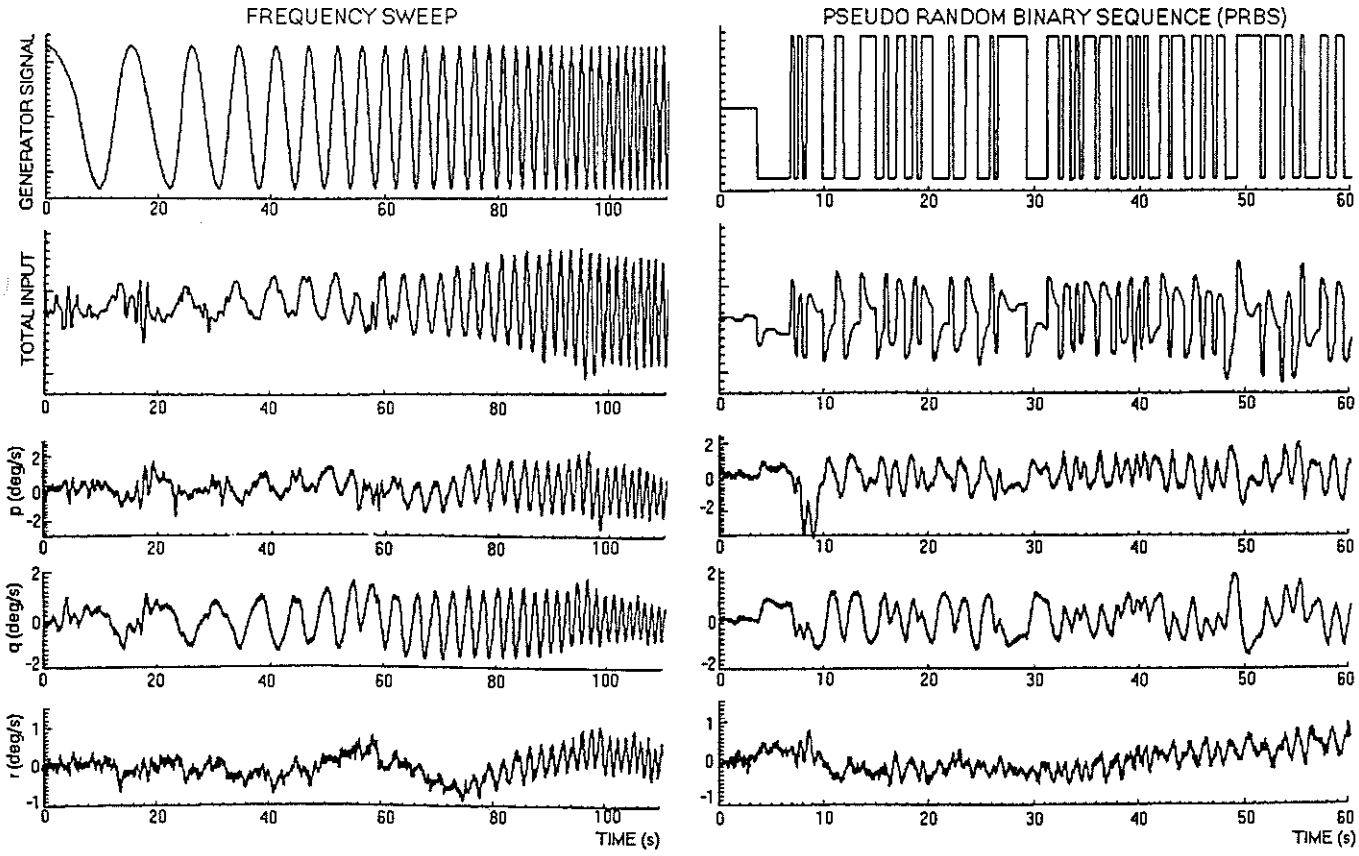

Figure 2: Comparison of input signal and associated rate responses (longitudinal stick, 100 Kt level flight)

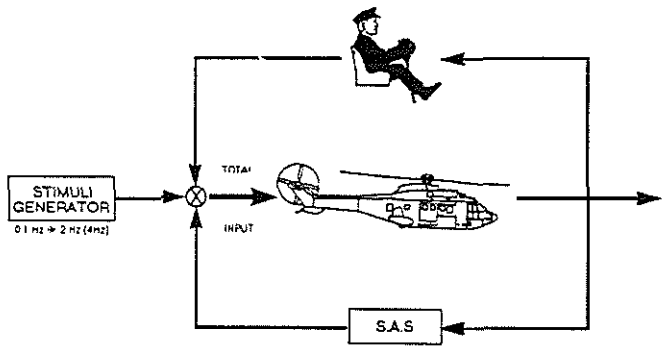

Figure 3: Contributions to control inputs for flight mechanics identification

Data processing

Flight test data was processed with an identification software developed by ONERA/CERT. This software is based on a multi-input / multi-output algorithm and provides the complete set of direct and cross-coupled transfer functions of a multi-dimensional system.

Associated with the identified transfer matrix, coherence function γ provides data regarding the validity of the identification. The coherence can be interpreted as a ratio between the estimated output spectrum (calculated with the estimated transfer function and the measured input) and the measured output spectrum.

$$\gamma_{,} = \sqrt{\phi_{y\underline{x}} \cdot \phi_{\underline{x}\underline{x}}^{-1} \cdot \phi_{\underline{x}y} \; / \; \phi_{yy}}$$

where:
- y = output scalar
- $\underline{X}$ = input vector
- $\phi_{\underline{x}y}$ = cross-spectral density vector
- $\phi_{\underline{x}\underline{x}}$ = co-spectral density matrix
- ϕ_{yy} = co-spectral density

The coherence function always is included between 0 and 1. The identified transfer function is considered correct when $\gamma > 0.8$, which means, amongst other things, that the linear behaviour assumption is well verified.

The coherence is calculated for each output and, consequently, will apply here to the four transfer functions of the same output. Plots on fig. 4 give the coherence function for the roll, pitch, yaw and vertical rates in level flight at 100 Kt for an input signal between 0.1 and 2 Hz. The results are good, except for the yaw response which is between 0.2 and 0.3 Hz approximately. This frequency range corresponds, in fact, to the low damping Dutch Roll mode. Pitch and roll responses also seem to be affected, but always stay above the acceptable 0.8 level.

AFCS influence and input signal selection

Close-loop identification is addressed in (3) where the main conclusions are:

- close-loop identification can lead to biased estimates of open-loop transfer functions in the presence of process noise,
- when the noise-to-signal ratio is limited, the error remains acceptable,
- for low to moderate process noise levels, the coherence function is a good indicator of the quality of the open-loop transfer function.

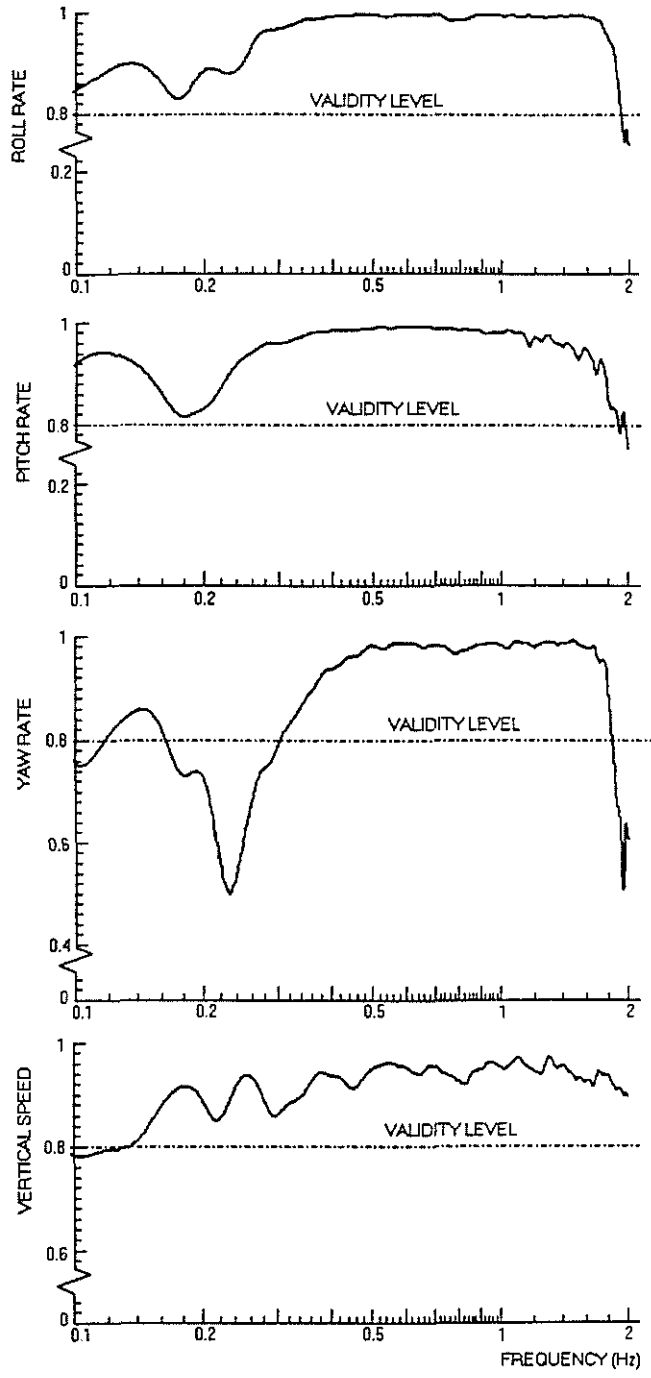

Figure 4: Coherence functions of the four outputs (100 Kt level flight - frequency sweep)

To limit the process noise level as much as possible, tests have been conducted in very calm atmospheric conditions. Coherence values have been checked and some tests have been repeated in different flights. This proved that the results were constant. In addition, some SAS OFF tests were performed using single frequency sinusoidal inputs during a 100 Kt level flight, where the use of SAS is not mandatory. Some points of the transfer functions were derived from those and proved to follow exactly the results of the close-loop identification.

Both frequency sweeps and PRBS have successfully been tested. Very similar results were obtained for transfer functions and coherence. No significant improvement can be attributed to PRBS. The results presented are all derived from frequency sweeps.

Corrections

Neither the servo-controls nor the measurement system are included in the S80 simulation model. Corrections of servo-control's transfer function and digital sensors time delay are thus cancelled out of the identification results.

To make the analysis easier, flight results were processed as if the mechanical linkage between the collective stick and the tail rotor pitch did not exist. The Super Puma data file has been changed accordingly. The results presented thus consider that the collective stick only acts on the main rotor's collective pitch and the pedal only commands the tail rotor's collective pitch (100% pedal range corresponding to the full tail rotor collective pitch range).

The S80 simulation model

Model description

ECF has been developing a generic rotorcraft simulation model called S80 since 1980. Its last version, based on a modular structure, is able to modelize any rotorcraft with the following elements:

- rotors (in fixed position or installed on a tilting nacelle),
- airframe (fuselage, fin, horizontal stabilizer, tilt-rotor wing...),
- engines (not considered in the results presented),
- landing gear (only for on-ground simulation and not used in this study)

Rotor model

Any rotor in the configuration being modelized can be represented either by a disk model or a blade element model. The latter is derived from the rigid blade version of the R85 rotor model presented in (4) and modified so as not to include trim calculations only, but also linearization and non-linear simulation. This model uses 2D airfoil characteristics measured in the wind tunnel as a function of the Mach number and angle of attack.

In this study, the blade element model with second order flap and lag degrees of freedom has been used for the main rotor, while the disk model with quasi-steady flapping was considered for the tail rotor. Since no engine model has been used, the main rotor RPM Ω is assumed to be constant (in helicopter axes).

In both the disk and blade element models, inflow is based on Meijer-Drees formulation, with a first order variation of the mean induced velocity.

Airframe model

The airframe is separated into elements and each element is modelled by a full set of 6 aerodynamic coefficients derived from wind tunnel data. When both angles of attack (α) and sideslip (β) are small (typically below 20°) measurements are made on a fine mesh of (α,β) range and transformed into polynomial expressions of α and β, thus providing some smoothing. Out of this small angles area, measurements are limited to some α-sweeps with constant β, and β-sweeps with constant α. A large angles model is derived from these measurements. A smooth transition from small to large angles is provided for in the calculation.

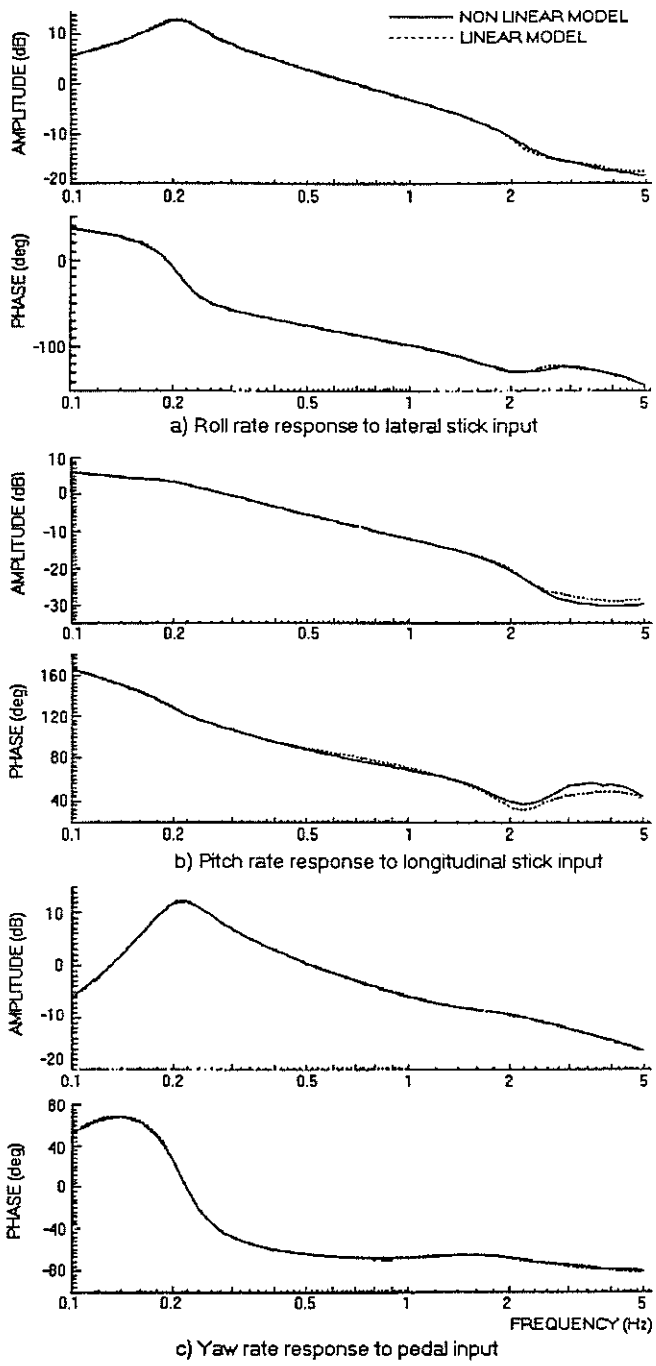

a) Roll rate response to lateral stick input

b) Pitch rate response to longitudinal stick input

c) Yaw rate response to pedal input

Figure 5: Bode plots comparison between non-linear and linear models - On-axis response (S80 calculations, 100 Kt level flight)

The effect of aerodynamic controls on the wing or tail surfaces (stabilator, fin rudder) can be included but is not needed for AS 332 L2.

Aerodynamic interactions between rotors and components of the airframe can be taken into account. Interactions models are derived either from flight or wind tunnel tests. In a single main rotor helicopter configuration, fuselage vertical drag at low speed, main rotor/fuselage and tail rotor/fin interactions are usually considered.

Linear model

The non-linear model can be linearized numerically with a small perturbation method. This provides a linear model with 22 states:

$$X = (u, v, w, p, q, r, \varphi, \theta, V_{\omega}^{MR}, V_{\omega}^{TR}, \beta_0, \beta_c, \beta_s, \dot{\beta}_0, \dot{\beta}_c, \dot{\beta}_s, \delta_0, \delta_c, \delta_s, \dot{\delta}_0, \dot{\delta}_c, \dot{\delta}_s)$$

Calculation of the transfer functions of the model

The S80 software has been modified to calculate the transfer functions of the helicopter starting from the linear or non-linear model.

The analytical solution $H(j\omega)=(j\omega.Id - A)^{-1}.B$ applies for the linear model, which only requires a very short calculation time.

When the non-linear model is considered, a time history simulation with harmonic input is first performed for each frequency ω and repeated on the four axes. The beginning of the simulation with the transient is dropped in order to consider the stationary forced response at ω frequency only. A Fourier analysis then provides the associated transfer function point for each input/output pair. Some SAS capability can be added, leading to a multi-input simulation which requires a linear system to be inverted to obtain single input-single output transfer functions. No process noise exists in simulation and inputs with very small amplitudes can be used. However, low frequencies require an extensive simulation time with a high helicopter drift risk in case of unstable behaviour and the use of the SAS may then become mandatory.

This easily implemented procedure calls for a rather expensive computation time, especially at the lowest scanned frequencies. No effort has been made to optimize this calculation: this non-linear approach is seldom used since linear calculation proved to give very comparable results. Particular attention must be paid to the amplitude of the signals in the non-linear case, especially when approaching the frequencies of the main rotor modes. Non-linearity like the lag damper behaviour can be significant in this frequency domain.

Some examples of comparison between non-linear and linear models are presented on fig. 5 (on-axis responses) and fig. 6 (off-axis responses) for a frequency range of 0.1 5 Hz. In fig. 5 the two curves are quite superimposed and it is sometimes difficult to separate them. These plots do not require too many comments: the fit between linear and non-linear models is excellent, for both on-axis and off-axis responses. This result differs significantly from already published data. In (5), the comparison between linear and non-linear models is good, but far from the one-curve plots of fig. 5. The different methods used to calculate the non-linear transfer functions can perhaps explain this phenomenon.

In previously published studies (5,6,7), non linear model transfer functions are obtained with exactly the same tools as the flight results. The simulation response to control frequency sweeps is first generated and then processed in the same way as flight data. The main advantage of this method is that both experimental and calculation results are seen in the same perspective: they are thus equally distorted and the errors

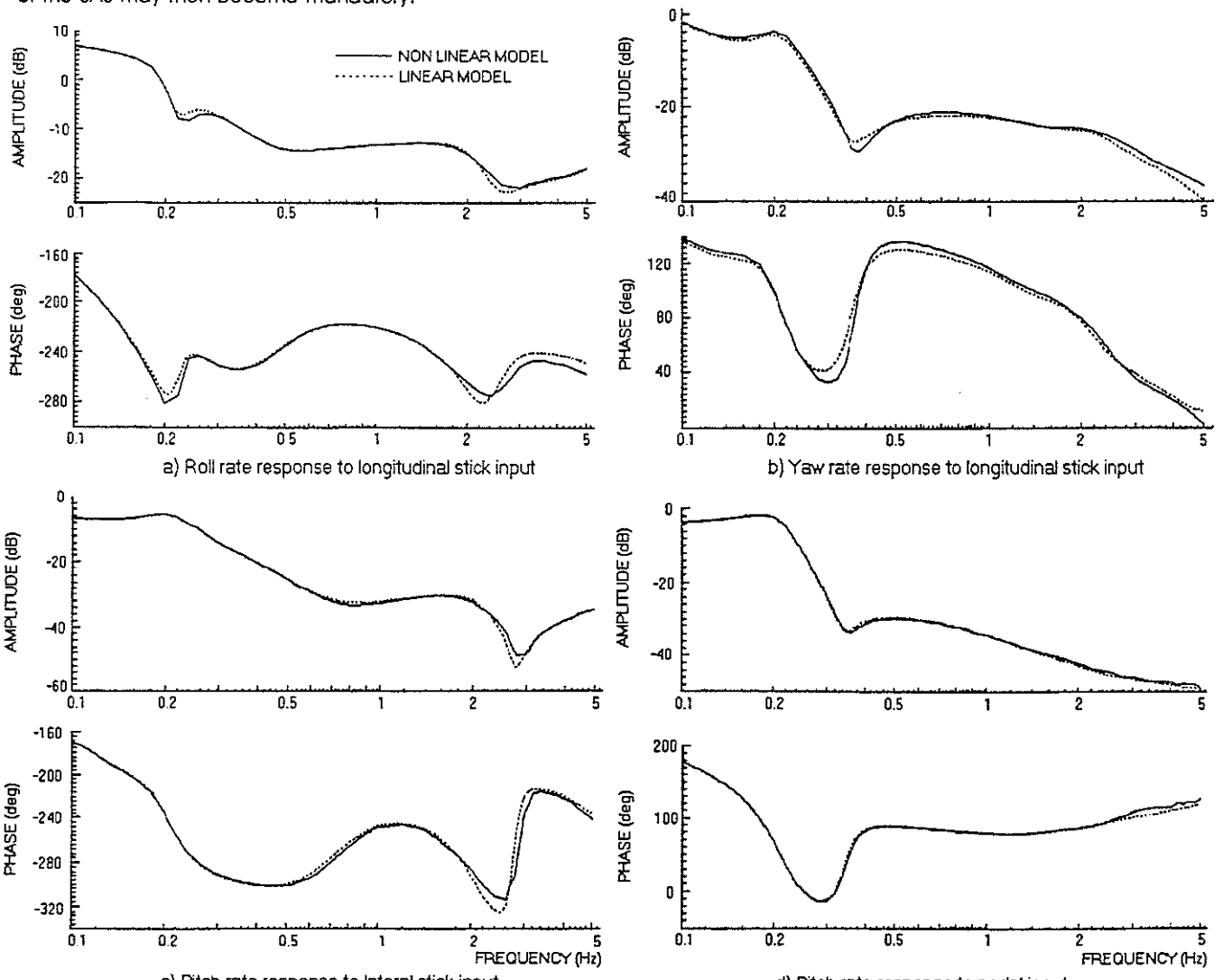

a) Roll rate response to longitudinal stick input

b) Yaw rate response to longitudinal stick input

c) Pitch rate response to lateral stick input

d) Pitch rate response to pedal input

Figure 6: Bode plots comparison between non-linear and linear models
Off-axis response (S80 calculations, 100 Kt level flight)

introduced by the identification method have a limited effect on the comparison outcomes. In the ECF procedure, two different identification methods are used for flight and simulation. The latter cannot be used for flight data but produces a very good fit between linear and non-linear models. These different methods can have a negative effect when comparing flight and simulation transfer functions because the origin of discrepancies can be a deficiency of either the model, or the identification method.

Following its experience, ECF applied the identification algorithm to linear simulation results with frequency sweep inputs which calculated transfer functions deviating from the analytical solution. This is particularly noticeable in the low frequency range, where the phugoid resonance peak is seriously underestimated when compared to the analytical solution.

These possible limitations of identification tools have to be borne in mind when looking at the comparisons. Fig. 5 however validates the calculation of transfer functions in the non-linear model. It also demonstrates that, for the considered amplitudes at least, there are no significant non-linear effects. Due to the high level of similarity between non-linear and linear transfer functions demonstrated in fig. 5 and fig. 6, all computations presented further in this paper will only relate to the 22 order linear model.

Results

The flight test envelope includes level flight from 100 Kt up to V_H and rate of climb/rate of descent variations at 100 Kt. A gross weight of approximately 7000 kg (15400 lb.), as well as neutral longitudinal and lateral CG, were retained for all tests. The results presented here mainly concentrate on the 100 Kt level flight case. Most of the conclusions would nevertheless be similar if derived from other AS 332 L2 experimental data.

Results are presented as Bode plots of the transfer functions considered in the test frequency range (0.1 - 2 Hz). Flight data are in full line and simulation results in dashed line whenever they are compared. The flight data will always be considered as the reference: when comparing phases, lead will thus mean that the simulation phase is higher than the flight phase, lag that it is lower.

What can be seen in transfer functions?

Prior to studying the results, it can be worth spending some time looking at fig. 5 and 6.

On-axis responses are the easiest to analyse. The low damping Dutch roll mode can be observed on both roll and yaw responses (0.2 Hz). The highly damped mode of longitudinal short period is not so apparent on pitch response (0.14 Hz), and the phugoid is outside the frequency range displayed. The most visible of the rotor modes on the airframe responses is the regressive lag mode (between 2 and 3 Hz).

In a multi-dimensional system, the same poles of the system are distributed in each transfer function. However, those poles that are not relevant to the dynamics of a response are compensated by zeros on the corresponding transfer function. In fact, this reciprocal cancellation depends on the amount of cross-coupling in the system (8). This cancellation is generally more efficient for on-axis than off-axis transfer functions (This is demonstrated in a simple case in the Appendix).

This can be seen on the off-axis transfer functions of fig. 6, where zeros frequencies do not exactly correspond to the poles frequencies. For example, in q/δ_{ped} (pitch rate response to pedal input), the Dutch roll mode appears at its natural frequency of 0.2 Hz but is compensated later by a zero at 0.35 Hz, although the same compensation can be considered perfect on the on-axis response q/δ_{lon} (pitch rate response to longitudinal cyclic).

On-axis response

100 Kt case

On-axis transfer functions are presented in fig. 7 for the nominal flight case (100 Kt).

Pitch rate response (7.b) is the best calculated with S80. The main deficiency of the model is a 1 - 2 dB overestimation of the amplitude within the whole frequency range. It slightly increases in the vicinity of the Dutch roll frequency (0.2 Hz), due to a small notch in the experimental curve which does not exist in the calculated data. This could be explained by a roll/pitch or yaw/pitch coupling higher in flight than it is in simulation. It will be further discussed with the influence of the trim airspeed.

Roll rate amplitude (7.a) is good in the (0.2, 0.7 Hz) range including the Dutch roll frequency, but underestimated at lower and higher values. The phase is good over 0.6 Hz, but differs at lower frequencies where a large lead can be seen (up to 40° at 0.1 Hz). Similar significant phase problems exist in the same frequency area, in both yaw (7.c) and vertical speed (7.d) responses.

The Dutch roll frequency can be seen on yaw transfer function, either through the amplitude peek or the phase shift, and is well calculated. The yaw amplitude is overestimated, especially in the vicinity of Dutch roll frequency. As the coherence is below the 0.8 confidence level in this area, the flight value can be questionable.

The vertical speed response to collective pitch is good in the upper frequency range only (over 0.6 Hz). In addition to the phase lead, an overestimation of the amplitude can be noted in the low frequency area (below 0.2 Hz).

On-axis results obtained with S80 simulation code are generally good, as already stated for similar models in previous studies (5,6,7,9). This is especially true in the upper frequency range (0.5 to 2 Hz), although some problems exist at lower values.

Influence of a change in airspeed on the on-axis pitch response

Reliable predictions of on-axis response invite us to check wether the model is able to apprehend minute effects. Fig. 8 shows the influence of a change in airspeed trim condition on the on-axis pitch rate transfer function. Fig. 8.a presents the flight data for both the 100 Kt (solid line) and 140 Kt (dashed line) cases, and fig. 8.b the corresponding calculation results. The coherence functions plotted in fig. 8.c validate the transfer functions identified in the whole frequency range.

The main change in the helicopter response between 100 and 140 Kt is limited to the low frequency range (0.1 to 0.3 Hz). This can be seen in both flight data and simulation results. In this area, the amplitude of the results identified decreases when the speed is increased and the notch previously noticed is deeper. A phase shift appears at the same time. This indicates an increase in lateral/longitudinal couplings moving the zero associated to the Dutch roll pole towards a lower frequency.

Simulation data present the same characteristics. The amplitude curve notch did not exist in the 100 Kt case and is well marked at higher speed, accompanied by a phase shift. The displacement of the zero associated to the Dutch roll pole is correctly represented by the model, which gives an indication

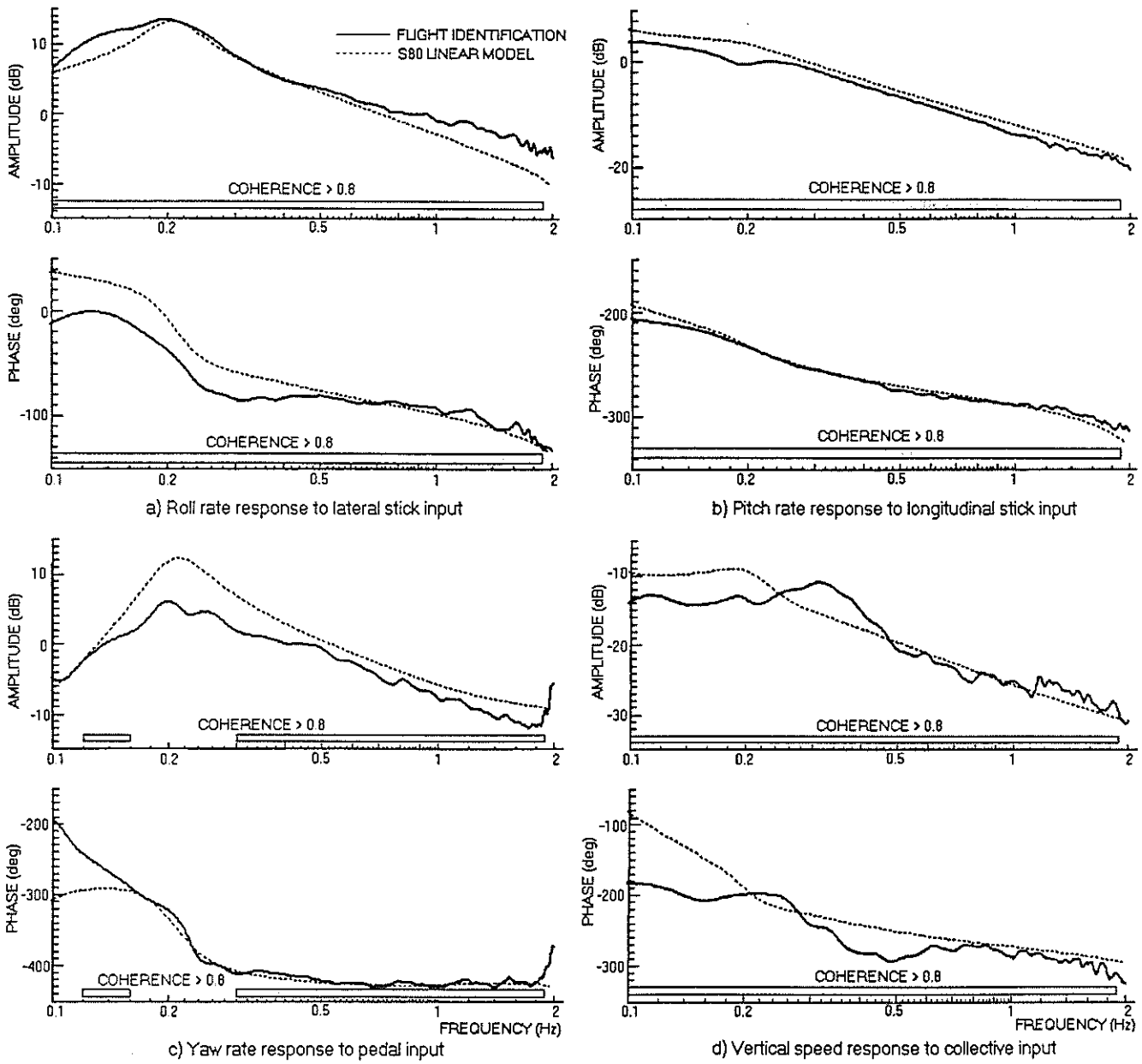

a) Roll rate response to lateral stick input

b) Pitch rate response to longitudinal stick input

c) Yaw rate response to pedal input

d) Vertical speed response to collective input

Figure 7: Comparison between calculated and flight-identified on-axis response (100 Kt level flight)

that the increase in lateral/longitudinal coupling is thus properly calculated.

It can be argued that the phase curves are somewhat different in the 140 Kt conditions: the phase shift is negative in the flight data and positive in simulation. The notches found in the amplitude curves prove that there is, in both cases, a zero placed at a lower frequency than the Dutch roll mode. When a zero cancels a pole, its phase shift is generally in the opposite direction than that due to the pole. This suggests an unstable Dutch roll mode in flight and a stable mode obtained by calculation. This hypothesis is confirmed when looking at the on-axis yaw response. The discrepancies in the phase curve of the 140 Kt on-axis pitch response thus result from a poor estimation of the Dutch roll damping, which is a common trend of mathematical models [1].

This example demonstrates that, on a highly coupled vehicle such as an helicopter, even on-axis responses are influenced by interaxis couplings. This is one of the reasons why simulation results compare better to flight data in the 0.5 to 2 Hz frequency range. Rigid body modes are lower, rotor modes higher and risks of couplings disturbance limited. However direct responses, including some coupling effects, are fairly represented in the S80 model.

Off-axis response

Cross couplings prediction is a known weakness of the current simulation models [2,10] and previous experience of time history comparisons with S80 demonstrated that improvements are required in this area. The use of identified transfer functions offers a more accurate insight in this area.

Roll/Pitch couplings

In fig. 9 are presented both pitch rate-to-lateral stick (9.a) and roll rate-to-longitudinal stick (9.b) transfer functions. The amplitude of the pitch response to lateral stick inputs is surprisingly close to the flight data, even if underestimated by 3-4 dB in the (0.2,0.7 Hz) range. This favourable result has to be tempered by an especially poor fit of the phase curve, despite the very large scale used. As poles and zeros of the transfer function act on both amplitude and phase, it is not easy to explain such a good result associated to such a poor one. It can however be observed on this off-axis response in any flight test case and this cannot be fortuitous.

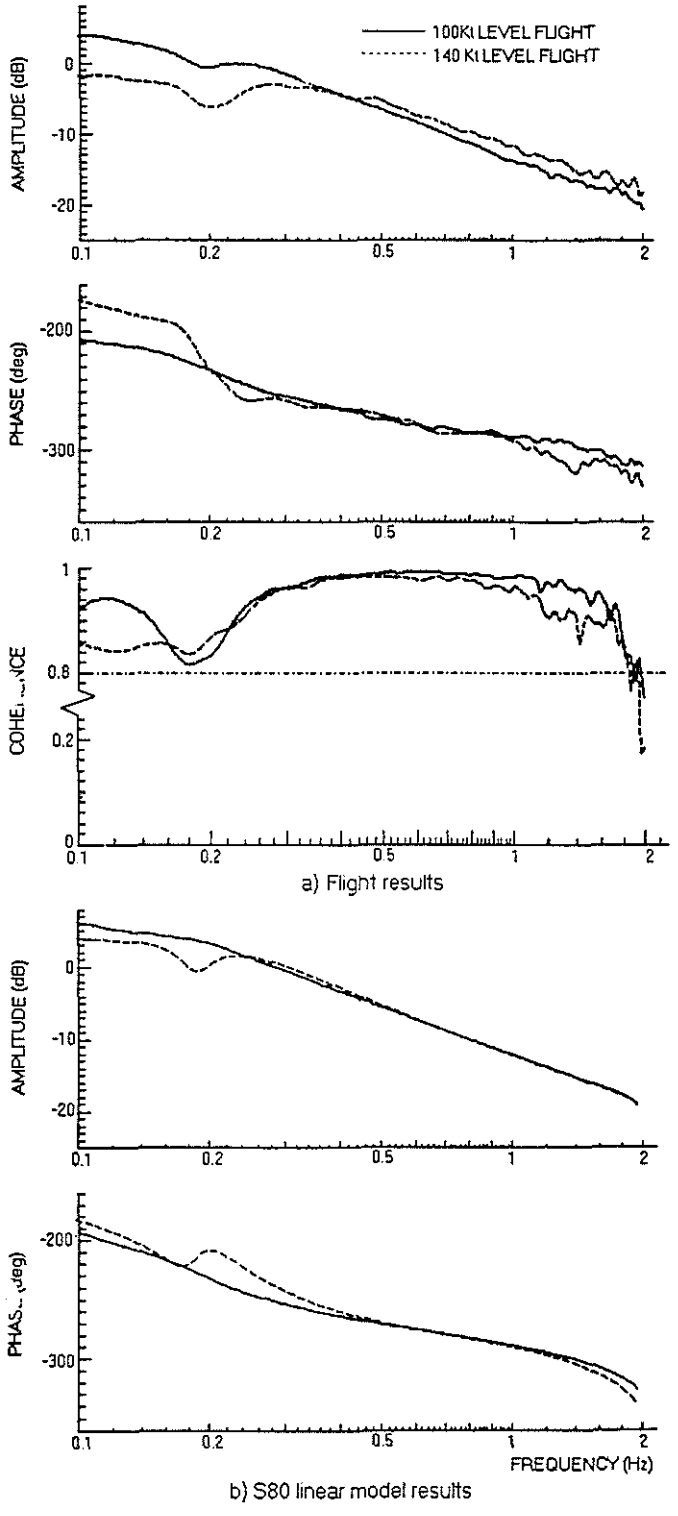

Figure 8: Pitch rate response to longitudinal stick input
Influence of a change in airspeed trim condition

An example of this type of behaviour can be found when comparing two second order models only differing by the sign of the damping (one is stable, the other unstable): they have the same amplitude curve but different phases, which produces a 360° difference at high frequencies. This generally happens when changing the sign of the real part of one pole or one zero of the transfer function. In the 100 Kt case and in this frequency range, signs of the poles real parts are identical in flight and in simulation. An erroneous zero is thus probable. This kind of error on a complex zero could explain 360° in the high frequency phase. However, the physical meaning of such an error is far from obvious!

The roll response to longitudinal stick is worse when amplitude is considered, but disparities are smaller on the phase curves. In any case, this calculated response is only mediocre: it does nor look too bad for low frequency (under 0.2 Hz) but has little to do with flight data at higher values, even when the maximum discrepancies (10 dB, 50°) are not outstanding.

On fig. 10, the roll response to both lateral (full line) and longitudinal (dashed line) stick inputs, as they were identified from flight data, have been plotted on the same graph (10.a). The low frequency range (below 0.25 Hz) excepted, both transfer functions are remarkably similar: amplitudes are shifted by a constant 10dB approx value, whereas phases present a constant 180° difference. Lateral and longitudinal stick have the same effect on roll response, which assumes that both controls have a common action on roll axis.

Swashplate control phase angle is one possible origin of such a behaviour. Both lateral and longitudinal stick inputs have a lateral cyclic pitch component. If the roll response to longitudinal cyclic pitch can be ignored, roll to lateral stick and roll to longitudinal stick transfer functions will be two different pictures from roll to lateral cyclic pitch response, with only different amplitudes.

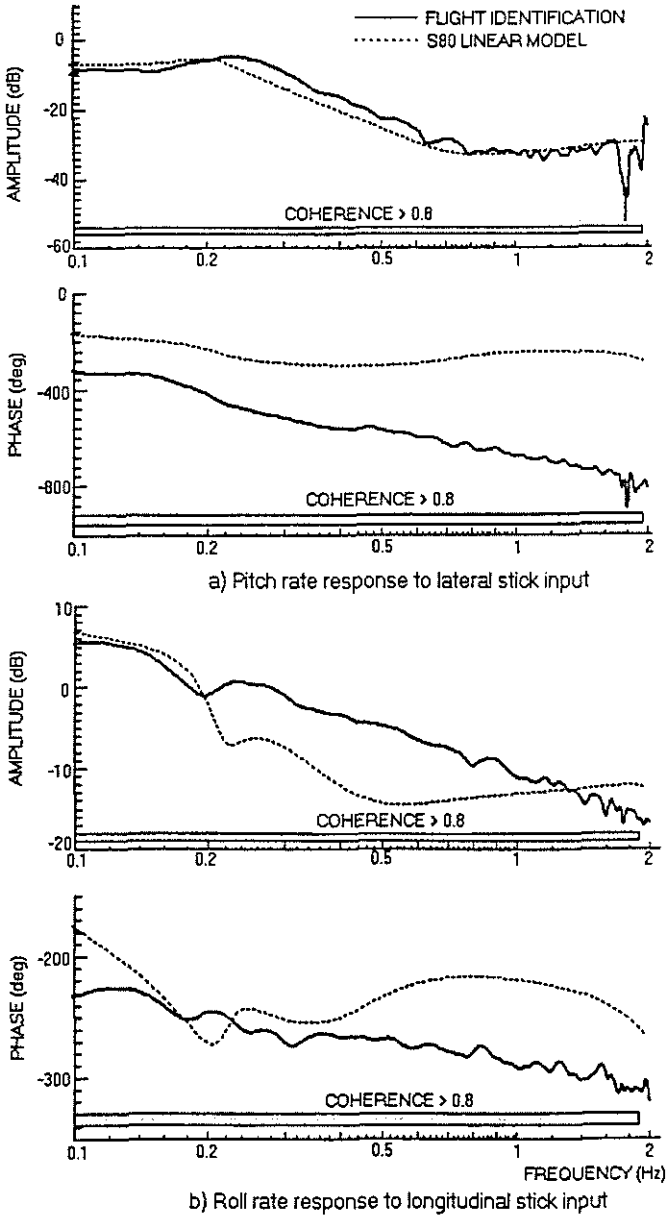

Figure 9: Comparison between calculated and flight-identifiedoff-axis response - Roll /Pitch couplings
(100 Kt level flight)

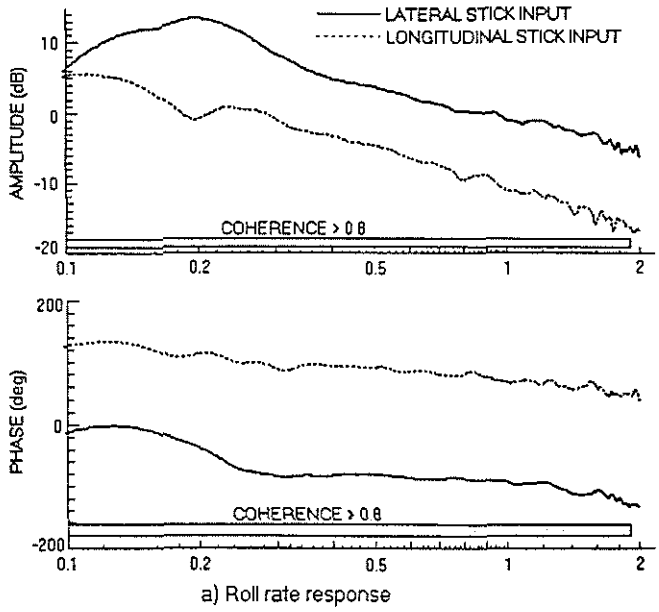

a) Roll rate response

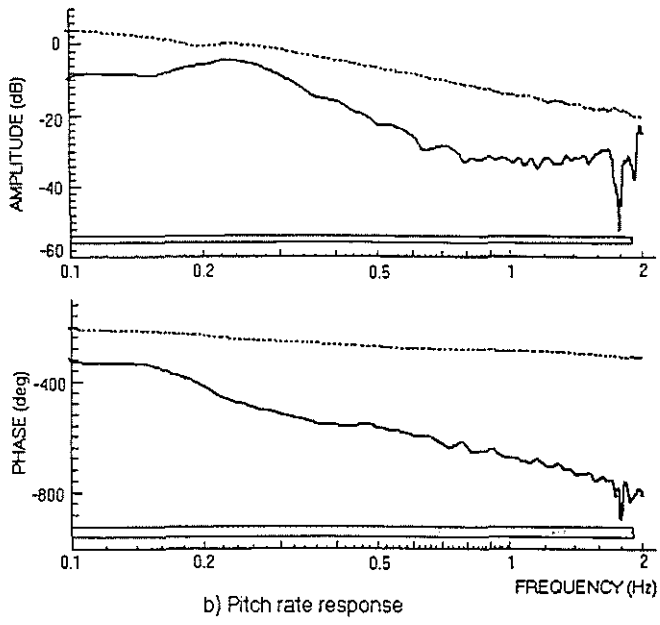

b) Pitch rate response

Figure 10: Comparison between responses to longitudinal and lateral stick inputs (100 Kt level flight)

There is no such resemblance on the pitch axis (10.b): the phase variation within the frequency limits of this study is much higher for the lateral than for the longitudinal input. This is however not inconsistent with the swashplate control phase influence. As the lateral cyclic pitch range is roughly half the longitudinal one and the pitch inertia is approximately five times the roll inertia, the pitch acceleration resulting from a 1% lateral stick input will only be one tenth of the roll acceleration resulting from a 1% longitudinal stick input and can be hidden by larger effects.

Simulation cannot readily explain the reason for the two similar roll axis responses: it does not come to the same result. The good fit of the on-axis transfer function and the problems with the off-axis one prove it. This topic will be investigated further in the model improvement efforts.

Roll/Yaw couplings

Fig. 11.a presents the pedal-to-roll rate and 11.b the lateral stick-to-yaw rate transfer functions. In both cases, simulation gives a fair estimation of the data identified. Shortcomings mainly related to amplitudes are:

- Roll response to pedal: an underestimation of amplitude in the Dutch roll vicinity (to be linked to a similar trend on the yaw response to the same input) and phase dissimilarity at low frequency,
- Yaw response to lateral stick input: an underestimation of amplitude by 3-5 dB in the whole frequency range.

Roll/Yaw responses to collective input

Roll response to collective plot (fig. 12.a) is fairly calculated and presents very comparable trends as regards vertical speed response to collective (fig. 7.d): phase lead below 0.2 Hz, overestimation of amplitude and phase lag between 0.3 and 0.6 Hz, proper fit beyond 0.6 Hz. On-axis response gives the variation of main rotor lift to collective input. It induces lateral force fluctuations due to the main rotor lateral flapping β_{1s}, and rolling moment through vertical main rotor/CG offset. This dominant effect and the lack of (disturbing) stabilizing area on the roll axis can explain the results reported.

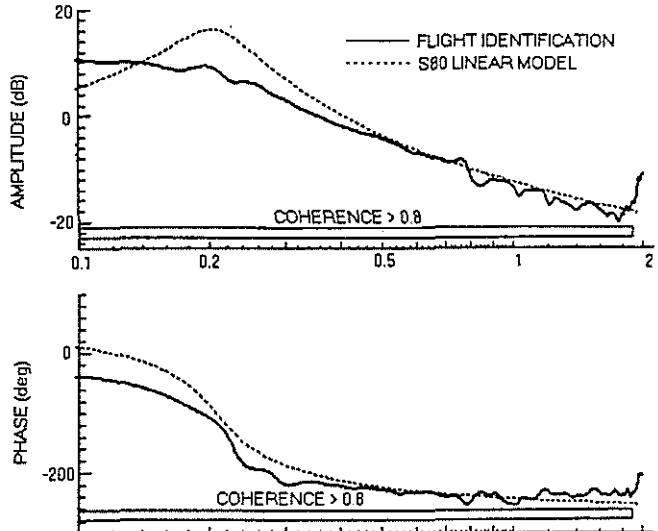

a) Roll rate response to pedal input

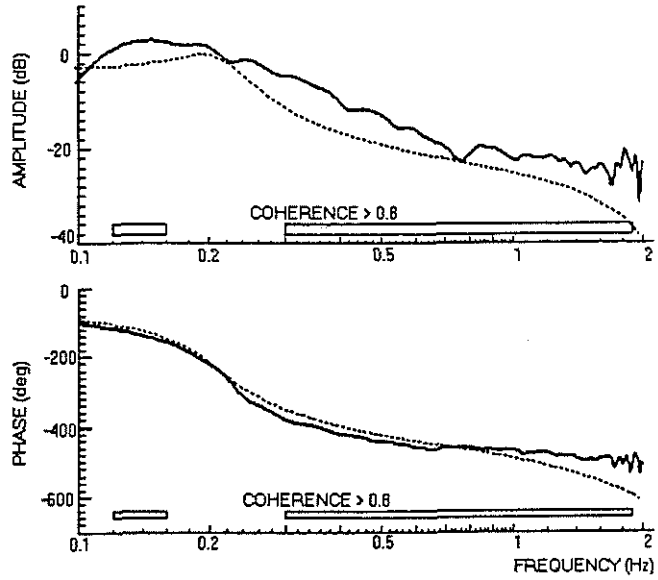

b) Yaw rate response to lateral stick input

Figure 11: Comparison between calculated and flight identified off-axis response - Roll /Yaw couplings (100 Kt level flight)

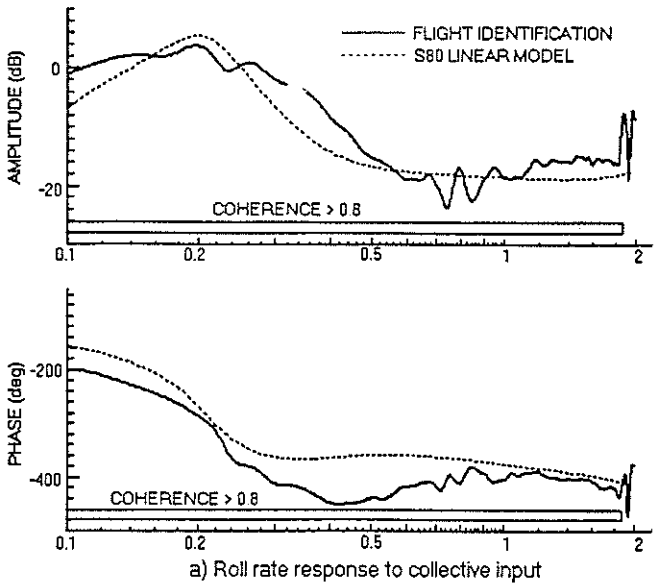

a) Roll rate response to collective input

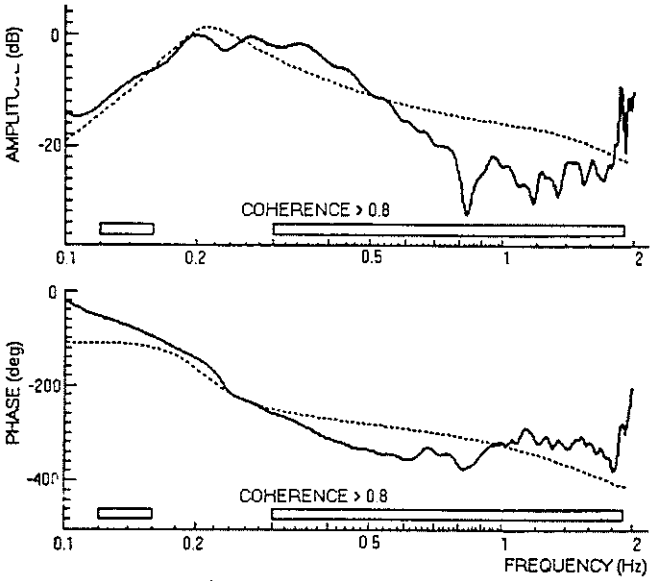

b) Yaw rate response to collective input

Figure 12: Comparison between calculated and flight identified off-axis response - Roll /Yaw responses to collective inputs (100 Kt level flight)

Fig. 12.b shows the yaw response to collective stick. Up to 0.6 Hz, it compares favourably to flight data and exhibits similar features as roll response in fig. 12.a, which can be an indication that it is induced by roll. Beyond 0.6 Hz, the fit is not so good. The "perfect" engine in the simulation could be responsible for poor high frequency fit.

Pitch/Yaw couplings

Criticism regarding interaxis couplings calculation by simulation models is totally merited in this area and it is difficult to find positive points in fig. 13. Only the high frequency part of pitch response to pedal (13.a) is acceptable. Yaw response to longitudinal cyclic (13.b) is definitely poor.

Analysis of the contributions of main elements to the transfer functions

Analysis method

Extracting the whole transfer functions matrix of an helicopter from flight records in a given flight case is a huge data reduction. The result however is a huge amount of data and it is not an easy task to determine the origin of the discrepancies between flight and simulation transfer functions. To obtain a better insight of physical phenomena, the contributions of the main elements to these transfer functions have been computed with S80.

The pitching moment acceleration can be written as:

$$\dot{q} = \frac{\mathcal{M}_q^{MR}}{I_{yy}} + \frac{\mathcal{M}_q^{TR}}{I_{yy}} + \frac{\mathcal{M}_q^{AF}}{I_{yy}} + \frac{I_{xz}}{I_{yy}}.(r^2 - p^2) + \frac{I_{zz} - I_{xx}}{I_{yy}}.p.r$$

The transfer function between one input and $\mathcal{M}_q^{MR}$ for example, divided by pitch inertia and integrated (amplitude divided by ω, 90° phase shift), will determine the influence of the main rotor on the pitch rate response to the considered input. It is easy to implement such a process in the calculation of the non-linear model transfer functions and this was done with the S80 software.

On-axis response results

On-axis responses results are shown in the (0.05, 5 Hz) range on fig. 14. The amplitude plot is the most important as it gives the predominance order.

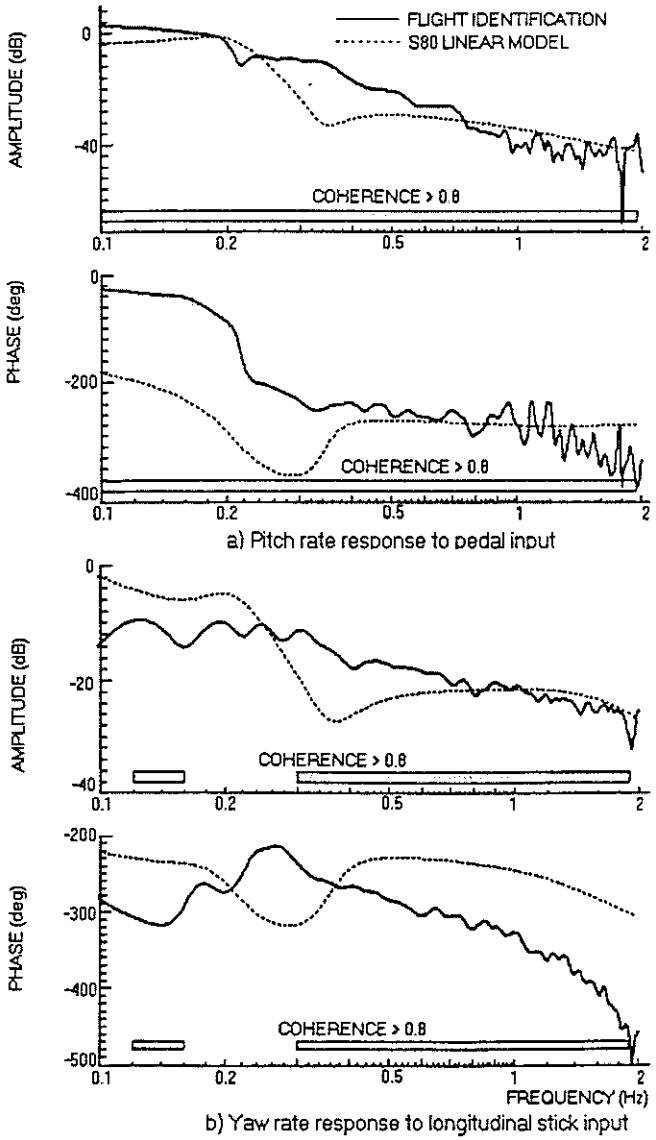

a) Pitch rate response to pedal input

b) Yaw rate response to longitudinal stick input

Figure 13: Comparison between calculated and flight-identified off-axis response - Pitch /Yaw couplings (100 Kt level flight)

Fig. 14.a is related to roll response. The airframe part is always very low, which is understandable, because there is no efficient stabilizer on the roll axis. The main rotor is dominant over 0.25 Hz: in this frequency range, the helicopter transfer function matches this element's contribution exactly. For lower frequencies, the main and tail rotor are both important, but are out of phase by about 180°. The total rolling moment is thus much smaller than any of the rotors contribution. Dutch roll corresponds to the frequency where both rotor phase curves intersect.

The pitch response is presented in fig. 14.b. In this case, the negligible effect is that of the tail rotor. The main rotor is predominant again over 0.1 Hz and compete with the airframe, which can be mainly attributed to the horizontal stabilizer, in the low frequency range.

As far as the yaw axis is concerned (fig. 14.c), tail rotor provides the major contribution at the higher frequencies, but all elements participate below the Dutch roll mode. In a large envelope, tail rotor and airframe components are out of phase by about 180°, which reflects the unstable yawing moment characteristics of the airframe.

Off-axis response results

Similar results are presented in fig. 15 and fig. 16 for off-axis response.

Fig. 15 is dedicated to roll/pitch couplings: roll response to longitudinal stick is presented in 15.a whereas 15.b shows pitch response to lateral stick. Both are governed by the main rotor contribution above 0.2 Hz. For lower frequencies, the main rotor still provides the major contribution to the roll response (15.a). The tail rotor and to a lower degree the airframe have a significant amplitude which comes in reduction to that of the main rotor for their phases differ by about 180°. The tail rotor does not contribute to low frequency pitch response (15.b) but the airframe (certainly through the horizontal stabilizer) is at the main rotor level.

Pitch/yaw couplings are shown in fig. 16. The tail rotor contribution to pitch response-to-pedal input (16.a) is dominant over 0.4 Hz but largely exceeded by those of the airframe and especially the main rotor in the low frequency range. Similarly yaw response to longitudinal stick (16.b) is essentially due to the main rotor beyond 0.4 Hz, while all contributions are significant at low frequencies.

Discussion

Table 1 summarises the results previously noted and gives, for all transfer functions related in fig. 14 to 16, the predominant elements within the frequency range.

A constant trend exists in all these transfer functions:

- Upper frequency range: from 0.1 - 0.4 Hz (depending on the transfer considered) up to the upper calculation limit, the contribution of the rotor where the input applied (i.e. the main rotor for stick inputs, the tail rotor for pedal inputs) exceeds by 20, and sometimes 40 dB, those of other elements.
- From the lower frequency calculation limit up to 0.1 - 0.4 Hz: more than one element is generally significant and the global rate response is often smaller than individual contributions.

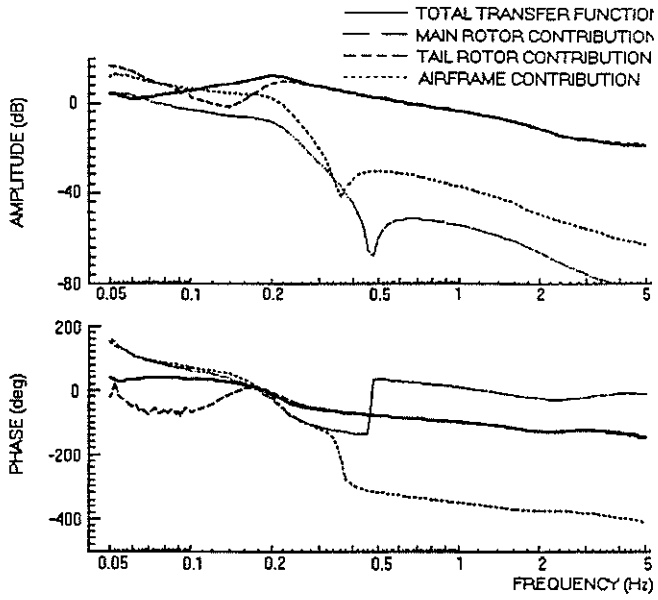

a) Roll rate response to lateral stick input

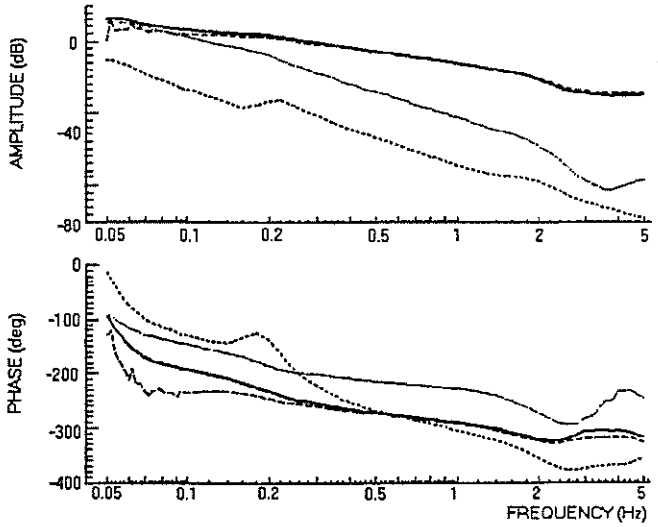

b) Pitch rate response to longitudinal stick input

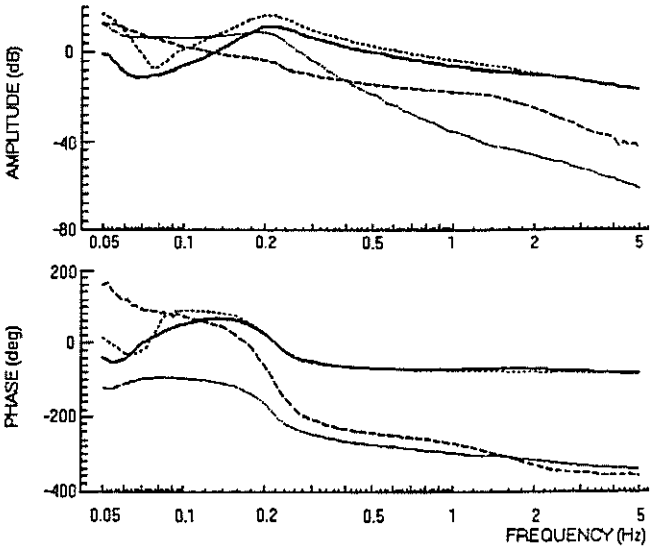

c) Yaw rate response to pedal input

Figure 14: Contributions of main elements to calculated transfer functions - On-axis response (100 Kt level flight)

A simple physical explanation can be given in the case of an on-axis response:

transfer function	frequency range (0.05 Hz, 0.1 Hz, 0.4 Hz, 5 Hz)		
p/δ_{lat}	MR,TR		MR
q/δ_{lon}	MR,AF		MR
r/δ_{ped}	MR,TR,AF		TR
p/δ_{lon}	MR,TR+AF		MR
q/δ_{lat}	MR,AF		MR
q/δ_{ped}	MR	MR,TR,AF	TR
r/δ_{lon}	MR,TR		MR

Table 1: Summary of main contributions to transfer functions

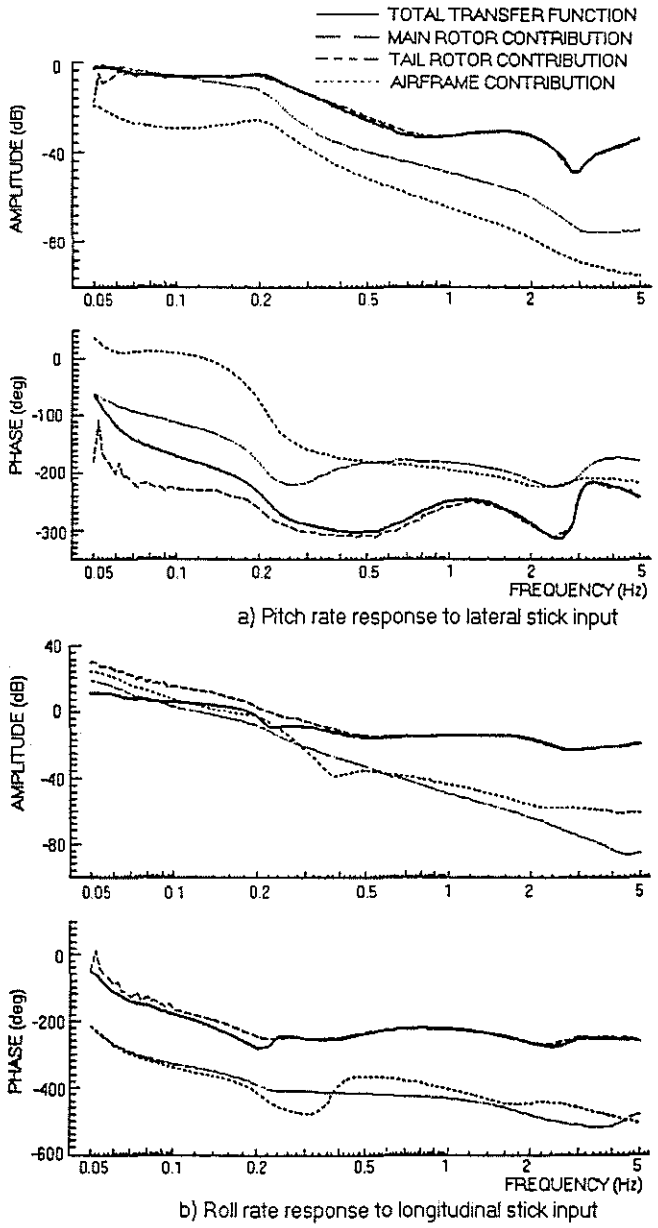

a) Pitch rate response to lateral stick input

b) Roll rate response to longitudinal stick input

Figure 15: Contributions of main elements to calculated transfer functions - Roll/Pitch couplings (100 Kt level flight)

1. Each individual contribution of the the helicopter elements is influenced by variations of state vector, but control input only affects the rotor where it is applied.

2. Constant amplitude input (when varying frequency) will, as a first approximation, provide forces and moments and, consequently, accelerations of an even magnitude. The velocity components and angular rates are the result of the integration of these accelerations of even magnitude and will thus decrease with frequency such as ω^{-1}.

3. The perturbations of the helicopter states are much reduced in the upper frequency range: the inputs are too rapid to induce a significant movement of the aircraft. Contributions from all elements, stimulated rotor excepted, are thus very limited at high frequencies.

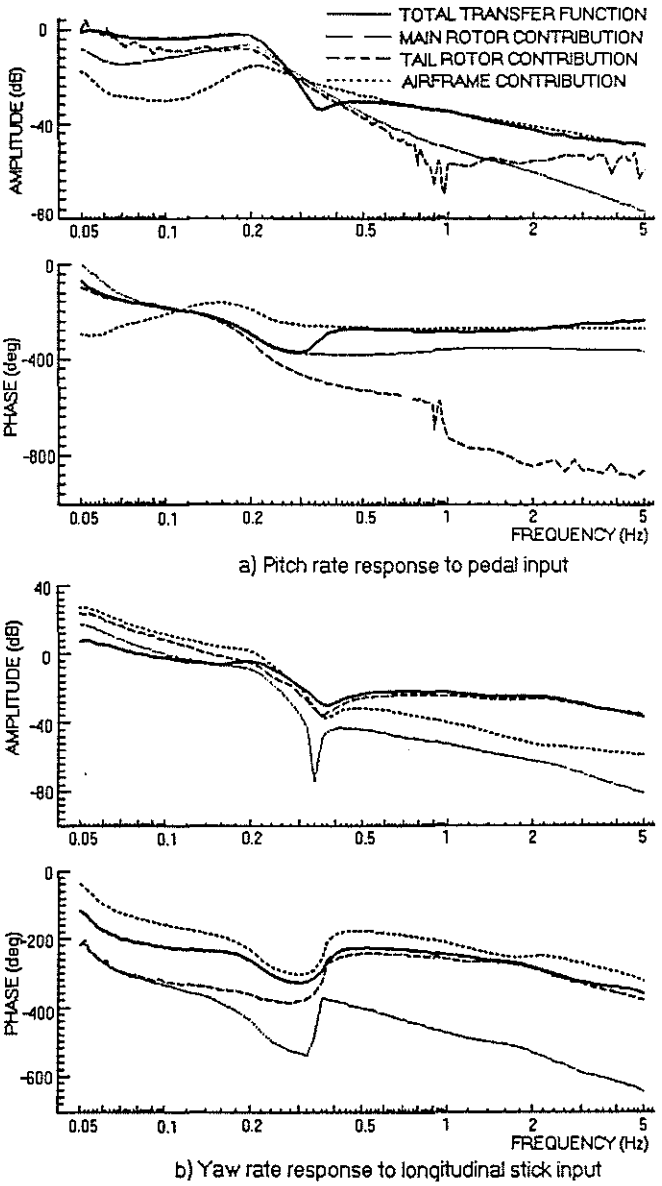

a) Pitch rate response to pedal input

b) Yaw rate response to longitudinal stick input

Figure 16: Contributions of main elements to calculated transfer functions - Pitch/Yaw couplings (100 Kt level flight)

This clarifies some key points in the comparison between computed and flight data extracted transfer functions:

- on-axis results are especially good in the upper frequency area, because they essentially reflect the main response of the excited rotor, which is not too poorly calculated,

- at low frequency, because of high variations in helicopter states, on-axis response is the combination of the contributions from various elements, and thus more difficult to compute,

- these two aspects also exist for off-axis response, but with an additional confusion: the primary response of the excited rotor is no longer considered, but only a coupling effect. When this coupling is directly linked to the main effect the off-axis response can be fairly well predicted (see, for example, roll moment due to collective, as previously discussed in off-axis results). When the link with the primary effect is less evident, the high frequency calculation can be wrong.

From this analysis, it can now be explainable why pitch response to pedal is better estimated for higher frequencies than yaw response to longitudinal stick:

- The tail rotor pitching moment comes mainly from the vertical force induced by the tail rotor lateral flapping β_{1s}. It is directly linked to tail rotor thrust which is the main parameter affected by pedal inputs. This high dependence on primary effect leads to a good fit (fig. 13.a) at high frequencies.

- The main rotor yawing moment is either due to torque or to lateral force through main rotor lateral flapping and main rotor/CG longitudinal offset. The connection between these factors and the main parameter governed by longitudinal stick, i.e. longitudinal flapping, is not obvious and explains the absence of fit in fig. 13.b.

Model modifications

Swashplate control phase

Swashplate control phase seems to be a very attractive way of adjusting roll to longitudinal cyclic and pitch to lateral cyclic responses. The direct and coupled effects are indeed respectively in the ratio of the cosine and sine of the swashplate control phase angle. It provides an influent tuning parameter for off-axis transfer functions without disturbing the on-axis pitch and roll responses, which were proved to be good.

The similarity between roll response to lateral stick and roll response to longitudinal stick illustrated in fig. 10 advocated some attempt to change this parameter in order to improve pitch/roll couplings. The results of this investigation are plotted on fig.17, with roll response to longitudinal cyclic on fig. 17.a and pitch response to lateral cyclic on fig. 17.b. The on-axis responses are not presented because they are not significantly altered by swashplate control phase change, at least within the limits considered here. Calculations have been conducted with swashplate control phase ranging from -15° to +15°, including the geometric +9° value (determined by a complete model of controls kinematics).

If roll amplitude is considered, the optimum swashplate control phase value is 0°: it gives a perfect fit between 0.25 and 1 Hz. From the phase point of view, negative values would be better. However, as they only slightly improve the phase curve and degrade the amplitude, 0° can be taken as an optimum swashplate control phase for roll response to longitudinal cyclic. The geometric 9° value, is quite far from this optimum, as already noted on fig. 9. This result must be linked to that of a previous ECF study using time history comparison and based on flight measured behaviour of AS 332 L2 following step inputs. It already concluded that 0° was the optimum swashplate control phase angle to calculate roll to longitudinal stick response with S80 in 100 Kt level flight.

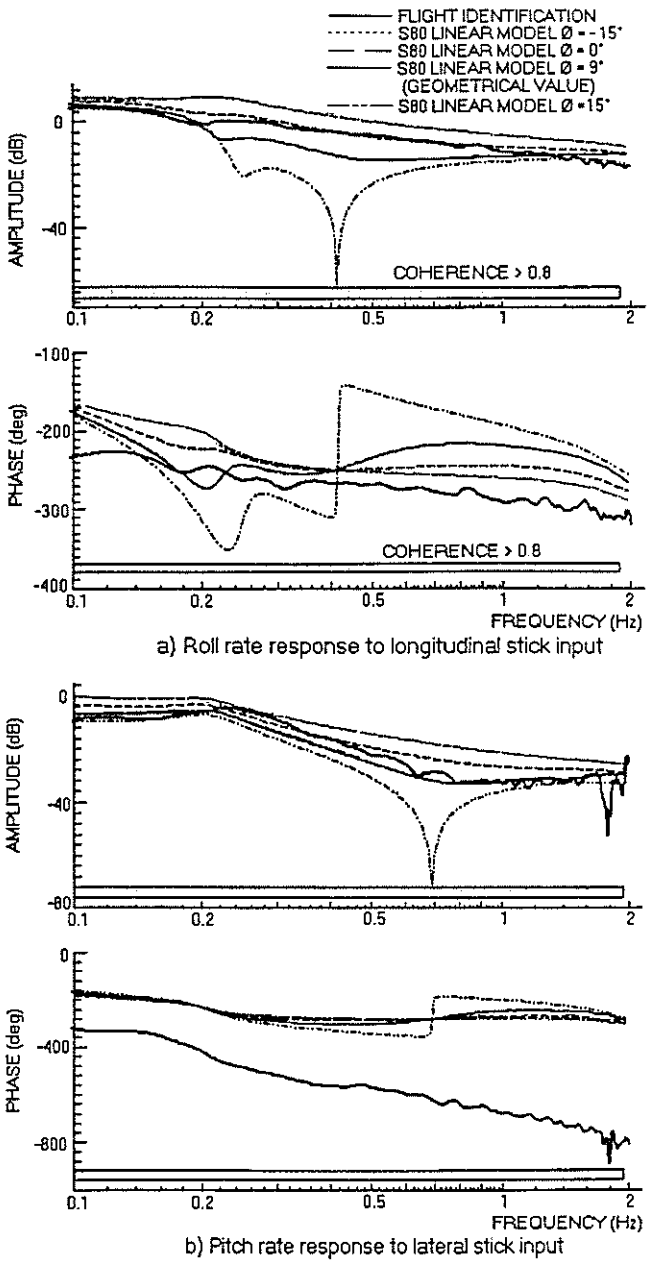

Figure 17: Calculated influence of the swashplate control phase angle on the Roll/Pitch couplings (100 Kt level flight)

The amplitude of pitch response to lateral stick was stated to be adequate with the geometric value of the swashplate control phase angle. It is confirmed by fig.17.b. The fit is not perfect and can be improved in the intermediate frequency range, but this has to be paid by a worsening in the high frequencies. The optimum for amplitude seems to be approximately 5°. The previously settled 0° roll optimum gives satisfactory result. It is not possible to set any optimum swashplate control phase value from the phase point of view: the influence of the range tested is quite negligible, at least in the flight data scale.

The swashplate control phase angle can be tuned to match the roll to longitudinal stick response (both in amplitude and phase) and pitch to lateral stick response from the amplitude point of view only. This conclusion is in agreement with a similar study based on tests performed on an isolated rotor in NASA Ames wind tunnel (9). A swashplate control phase value was identified and, once fed into a rotor model, proved to give good results for on-axis responses and roll response to longitudinal cyclic. Pitch response to lateral cyclic was "less satisfactory". (9) also reports a similar attempt to tune swashplate control phase angle in a UH-60 simulation model in order to match measured roll response to longitudinal cyclic in hover, which was unsuccessful. The present study seems to invalidate

the explanation of this problem by a difference between "shaft fixed" behaviour as in the wind tunnel and "moving shaft" behaviour as in flight.

The swashplate control phase angle is a valid means to improve the S80 response to longitudinal stick inputs in one flight case. It is doubtful wether a single value can do that within the whole flight envelope. S80 roll response to a longitudinal stick step with 0° swashplate control phase angle is good in the vicinity of 100 Kt only. This needs to be confirmed with an extensive analysis of the available results. In any case such an "adjustment", even if useful, is not very satisfying in a physical model.

Lag damper characteristics

It became obvious during AS 332 L2 development that some modelling problem existed in the high frequency domain. Flight tests demonstrated that the autopilot destabilized the lag regressive mode, which was not predicted by simulation.

As this phenomenon mainly occurs in high speed case, identification tests were performed at 140 Kt level flight. The frequency range of interest was shifted up to 4 Hz in order to capture the lag regressive mode, which frequency is about 3 Hz for AS 332 L2. The roll response to lateral stick input illustrates this problem and is presented on fig. 18.

The coherence function is under the 0.8 level at frequencies below 0.25 Hz. The stimuli generator did not begin sweeping at such a low frequency. The identified transfer function is questionable in this area. However, the low frequency results are of little interest in this paragraph.

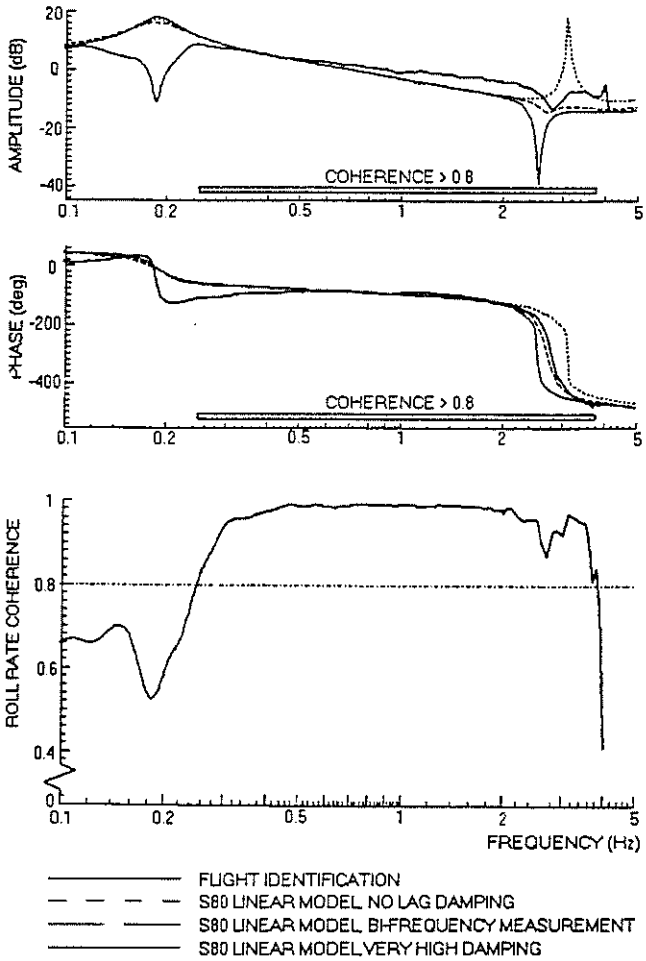

Figure 18: Calculated influence of lag damper characteristics on roll rate response to lateral stick input (140 Kt level flight)

A notch in the amplitude curve at about 3 Hz can be observed, accompanied by a negative 360° phase shift. It is the evidence of the lag regressive mode. Such a behaviour is typical of a transfer function pole, followed by a zero. Both induce a negative change in phase, which means that the pole is stable and the zero has a positive real part.

First simulation results were far from the experimental curve and the notch was much less marked, at a slightly lower frequency. The lag damper characteristics being suspected, calculations with extreme variations of these parameters were made as in (11); the results are also plotted in fig. 18. Without lag damping, the notch is changed into a bump. It appears at a higher frequency, where the phase shift is equally moved. With a very stiff damper, the effect is in the opposite direction: the notch becomes deeper and moves toward lower frequencies. This behaviour reflects the displacement of the zero with respect to the pole: starting almost at the same frequency, it moves beyond when damping is reduced and sets to a lower frequency when damping is increased.

The flight data are within these two calculations with extreme characteristics. If the underestimation of this transfer function amplitude, already noticed in the 100 Kt case, is not considered. It seems likely that damper characteristics exist that allow the S80 software to match flight measurements.

An empirical adjustment could perhaps have been made, but was of little interest to improve prediction capabilities. The method of measurement of elastomeric lag damper characteristics has been reconsidered. They are derived from rig measurements under harmonic solicitations at the main rotor rotation frequency. It allows calculating sizing damper loads, which are mainly 1/rev. In the flight conditions where lag regressive mode emerges, the damper is subject to harmonic solicitations at both 1/rev and first lead - lag frequency. New rig measurements were conducted, closer to flight conditions, with both harmonic inputs superimposed. The damper characteristics determined from these tests were fed into the simulation model, and results are presented in fig. 18. They are very close to flight data. Even if the amplitude notch is somewhat underestimated in the calculation, the phase curves are well merged with only a slight error in the frequency where the 360° shift occurs.

This example demonstrates that simulation data are at least as much significant as models are. A fair prediction of the phenomenon can be obtained, at the cost of additional rig tests suited to the damper working conditions. It is not quite appropriate because the damper data need to be adapted to the flight case and to the purpose of calculations. The next step will be to acquire a better understanding of the damper behaviour and establish a unique model valid throughout the flight envelope.

Conclusions

A validation study of a physical helicopter simulation model has been reported, using non parametrical frequency domain identification results.

- SAS ON identification tests in an AS 332 L2 helicopter and follow-up data processing were successfully performed in an industrial environment.
- The S80 simulation model was modified in order to calculate the helicopter transfer functions; both linear and non-linear models perfectly fit in the frequency range considered.
- On-axis responses only present very limited deficiencies and can even reflect changes in couplings as they are in flight.
- Off-axis results range from good to poor.
- An analysis of the contributions of the main helicopter elements to the transfer functions shows that the rotor plays the largest part at high frequency where the input is introduced.
- Tuning the swashplate control phase angle allows matching roll response to longitudinal stick but has little influence on pitch response to lateral stick. A large phase lag exists in flight transfer function which is not represented by the model.
- Lag damper characteristics measured with solicitations closer to those encountered in flight allow giving a fine representation of lag regressive mode.

Three years after the AGARD FMP Working Group 18 publication on Rotorcraft System Identification, which objective was "*to provide an overview and expertise to industry for... increased utilization of this modern flight test tool*", the main conclusion of this study can be that ECF has been convinced and plans to use at least non parametrical identification methods in any future helicopter development.

Acknowledgments

The authors are grateful to STPA (Service Technique des Programmes Aéronautiques) and DRET (Direction des Recherches Etudes et Techniques) who finance this research.

They also thank E. Godard and F. Sandri from ECF as well as B. Gimonet from CERT/DERA for their precious help with the flight data processing.

References

(1) G.D. Padfield, R.W. DuVal "Application Areas for Rotorcraft System Identification: Simulation Model Validation", AGARD LS 178 (Rotorcraft System Identification, October 1991

(2) H.C. Curtiss, Jr, "On the Calculation of the Response of Helicopters to Control Inputs", paper presented at 18th European Rotorcraft Forum, 1992

(3) M.B. Tischler, "Frequency-Response Identification of XV-15 Tilt-Rotor Aircraft Dynamics", NASA TM 89428, May 1987

(4) M. Allongue, T. Krysinski, "Validation of a New General Aérospatiale Aeroelastic Rotor Model Through the Wind Tunnel and Flight Test Data", paper presented at 46th Annual National AHS Forum, 1990

(5) F.D. Kim, R. Celi, M.B. Tischler, "High-Order State Simulation Models of Helicopter Flight Mechanics", paper presented at 16th European Rotorcraft Forum, 1990

(6) C.P. Beck, J.D. Funck, Jr, "Development and Validation of a Seahawk Blade Element Helicopter Model in Support of Rotorcraft Shipboard Operations", paper presented at RAS Conference on Rotorcraft Simulation, may 1994

(7) M.G. Ballin, M.A. Dalang-Secrétan, "Validation of the Dynamic Response of a Blade Element UH-60 Simulation Model in Hovering Flight", paper presented at 46th Annual National AHS Forum, 1990

(8) B.L. Stevens, F.L. Lewis, "Aircraft Control and Simulation", Wiley Interscience, 1992

(9) M.B. Tischler, J.T. Driscoll, M.V. Cauffman, C.J. Freedman, "Study of Bearingless Main Rotor Dynamics from Frequency-Response Wind Tunnel Test Data", paper presented at AHS Aeromechanics Specialists Conference, January 1994

(10) J.G. Yen, J.J. Corrigan, J.J. Schillings, P.Y. Hsieh, "Comprehensive Analysis Methodology at Bell Helicopters: COPTER", paper presented at AHS Aeromechanics Specialists Conference, January 1994

(11) T.T. Kaplita, J.T. Driscoll, M.A. Diftler, S.W. Hong, "Helicopter Simulation Development by Correlation with Frequency Sweep Flight Test Data", paper presented at 45th Annual National AHS Forum, 1989

Appendix: Influence of Interaxis Couplings on Transfer Functions Zeros

Consider a simple 2 inputs, 2 outputs system, represented by a linear model:

$$\dot{X} = A.X + B.U$$

$$A = \begin{pmatrix} a_{11} & a_{12} \\ a_{21} & a_{22} \end{pmatrix} \quad \text{and} \quad B = \begin{pmatrix} b_{11} & b_{12} \\ b_{21} & b_{22} \end{pmatrix}$$

The transfer functions can be calculated analytically by

$$H(s) = (s.Id - A)^{-1}.B$$

$$(s.Id - A)^{-1} = \frac{1}{\det(s.Id - A)} \cdot \begin{pmatrix} s - a_{22} & a_{12} \\ a_{21} & s - a_{11} \end{pmatrix}$$

with

$$\det(s.Id - A) = (s - a_{11}).(s - a_{22}) - a_{12}.a_{21}$$

With respect to the uncoupled model ($a_{12} = a_{21} = 0$), the poles (a_{11}, a_{22}) are changed into ($a_{11}-\varepsilon$, $a_{22}+\varepsilon$) with $\varepsilon = \frac{a_{12}.a_{21}}{a_{11} - a_{22}}$, if a_{11} and a_{22} are not too close together and if inter-axis couplings are only second order terms, i.e. if

$$a_{12}.a_{21} \ll a_{11} - a_{22}$$

Assuming that neither matrix B elements nor matrix A eigenvalues are zero, the transfer functions relative to X1 output can be written as:

$$\frac{X_1}{U_1} = b_{11} \cdot \frac{s - a_{22} \cdot \left(1 + \frac{a_{12}}{a_{22}} \cdot \frac{b_{21}}{b_{11}}\right)}{(s - a_{11} + \varepsilon).(s - a_{22} - \varepsilon)}$$

$$\frac{X_1}{U_2} = b_{12} \cdot \frac{s - a_{22} \cdot \left(1 + \frac{a_{12}}{a_{22}} \cdot \frac{b_{22}}{b_{12}}\right)}{(s - a_{11} + \varepsilon).(s - a_{22} - \varepsilon)}$$

Symmetrical formula would describe X2 transfer functions. This writing proves that coupling terms in matrix A (a_{12},a_{21}) move the zeros away from the poles of the uncoupled system. This effect is usually smaller on the on-axis transfer function where it is the product of two coupling to direct derivatives ratios on both state and control terms ($\frac{a_{12}}{a_{22}} \cdot \frac{b_{21}}{b_{11}}$) than on the off-axis transfer function, where the control term ratio is inverted.

When state coupling terms are weak, zeros are only moved away from the pole by a small distance. As a first approximation, the zero term in the numerator cancels the pole term in the denominator and the off-axis pole no longer appears in the transfer function. When couplings are weak, the off-axis modes are not visible on the on-axis transfer function. That means, for example, that if lateral to longitudinal couplings are weak, Dutch roll mode cannot be seen on the longitudinal stick to pitch rate transfer function.